Inorganic nanotubes and fullerene-like nanoparticles

R. Tenne[a)]
Department of Materials and Interfaces, Weizmann Institute of Science, Rehovot 76100, Israel

(Received 20 April 2006; accepted 25 May 2006)

We have proposed in 1992 that nanoparticles of layered compounds will be unstable against folding and close into fullerene-like structures and nanotubes (IF). Nanotubes and fullerene-like structures were prepared from numerous compounds with layered and recently also non-layered structure by various groups. Much progress has been achieved in the synthesis of inorganic nanotubes and fullerene-like nanoparticles of WS_2 and MoS_2 and many other metal dichalcogenides over the last few years. Substantial progress has been accomplished in the use of such nanoparticles for tribological applications and lately for impact resilient nanocomposites. These tests indicated that IF-MoS_2 and IF-WS_2 are heading for large scale applications in the automotive, machining, aerospace, electronics, defense, medical and numerous other kinds of industries. A few products based on these nanoparticles have been recently commercialized by "ApNano Materials, Inc". Novel applications of inorganic nanotubes and fullerene-like nanoparticles in the fields of catalysis; microelectronics; Li rechargeable batteries; medical and opto-electronics will be discussed.

I. INTRODUCTION

The discovery of C_{60}-the fullerene molecule with the highest symmetry and the most stable one of this series[1] in 1985 and the later discovery of carbon nanotubes[2] has established a new paradigm in chemistry. A new field of nanomaterials with polyhedral (hollow) nanostructures was thus born. Chemical bonding in general does not favor hollow spaces, which explains the initial reluctance to accept the notion of fullerenes. This reluctance was diffused once large amounts of C_{60} were purified and its nuclear magnetic resonance (NMR) spectrum proved its structure unequivocally in 1990.[3] Graphite is a quasi-two-dimensional (2D) (layered) compound consisting of molecular sheets arranged in a honeycomb lattice, i.e., (3-fold) sp^2 bonded carbon atoms. These graphene sheets are stacked together by weak van der Waals forces. Graphite is the most stable polymorph of carbon in ambient conditions, but it transforms under a pressure of about 1.7 GPa to diamond, which is a carbon lattice made of sp^3 (4-fold) bonded atoms. In the nano-size regime, however, the flat graphitic sheets (graphenes) become unstable due to the abundance of 2-fold bonded carbon atoms on the rim of the molecular sheet. This instability induces folding of the molecular graphene sheets into a closed-cage structure. The elastic energy of folding is thus more than compensated by the absence of dangling bonds of the rim atoms. Polyhedral carbon structures thus become the thermodynamically favorable form of carbon in the nanoscale. When 12 pentagonal rings occur in the carbon nanocluster, it closes onto itself and forms a hollow (polyhedron) structure, i.e., a fullerene. Forming nanotubes involves much less strain since the folding of the graphene sheet occurs in one direction only. To close this one-dimensional (1D) hollow nanostructure, six pentagons are disposed at each end of the nanotube to form a hemispherical cap on each side of the nanotube.

In 1992 it was hypothesized[4] that the propensity of graphite to form polyhedral structures is not limited to carbon. In fact, this property is likely to occur in nanoparticles of any compound with layered structure. Early hints to this instability and the existence of MoS_2 nanotubes and fullerene-like structures existed before.[5,6] Figure 1 shows the lattice of a nanocluster of MoS_2, emphasizing the difference between fully bonded bulk atoms and rim atoms with dangling bonds. Therefore, it is believed that the formation of closed polyhedra (fullerene-like structures) and nanotubes is a generic property of (2D) layered materials.[4,7,8] These structures were termed inorganic fullerene-like materials (IF). Multilayer polyhedra (onions or nested structures) and

[a)]Address all correspondence to this author.
e-mail: reshef.tenne@weizmann.ac.il
This author was an editor of this focus issue during the review and decision stage. For the *JMR* policy on review and publication of manuscripts authored by editors, please refer to http://www.mrs.org/jmr_policy
This review article is based on the author's 2005 MRS Medal talk titled "Inorganic Nanotubes and Inorganic Fullerene-Like Materials: From Concept to Applications," presented at the 2005 MRS Fall Meeting on November 30, 2005.
DOI: 10.1557/JMR.2006.0354

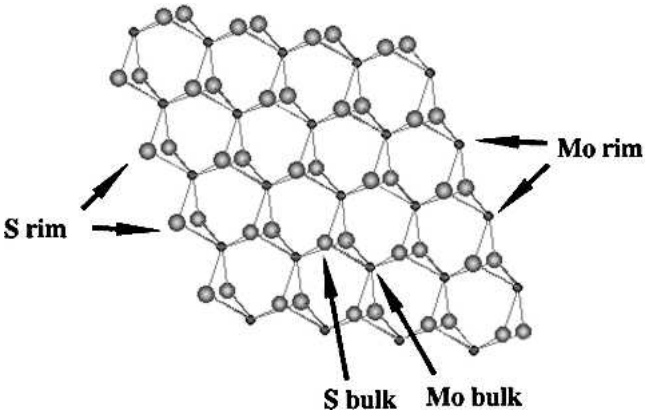

FIG. 1. Schematic drawing of MoS_2 nanocluster from the [001] direction. Note that while the bulk Mo and S atoms are 6-fold and 3-fold bonded, respectively, the rim atoms are 4-fold and 2-fold bonded only, making the planar nanostructure chemically unstable and forcing it to fold and close onto itself.

nanotubes make also part of the IF family and in fact might be the most stable of all IF structures. Figure 2 shows a transmission electron microscope (TEM) image of (a) a multiwall MoS_2 nanoparticle with fullerene-like structure and (b) three multiwall WS_2 nanotubes. The existence of IF structures was confirmed through various studies during the last few years. Nanotubes and fullerene-like nanoparticles of various 2D compounds have also been studied extensively through theory in recent years. These observations suggest that indeed the IF phase makes part of the phase diagram of elements, which form layered compounds, like Mo and S, or Ni and Cl.[9,10] If the otherwise planar crystallites are not allowed to grow beyond a certain size (less than, say, 0.2 μm), the closed cage phase becomes the thermodynamically favorable state. Globally however, the IF phase is less stable than the bulk 2D material, which often comes in the form of platelets.

Practically, the synthesis of IF phases proved to be exceedingly difficult, if not almost impossible in several cases.[9–11] These difficulties and their consequences will be discussed in the present text as well. X-ray diffraction (XRD) is usually used in elucidation of the crystalline structure of bulk materials. The synthesis and structural elucidation of IF materials rely primarily on TEM[12] and its associated techniques, like electron diffraction (ED), energy dispersive x-ray spectroscopy (EDS), and more recently, electron energy loss spectroscopy (EELS).[11]

Nanotubular structures from various three-dimensional (3D) compounds, like GaN,[13] AlN,[14] ZnS,[15] and many others were also recently reported. A clear distinction holds between nanotubular structures obtained from isotropic (3D) and layered (2D) compounds. Two-dimensional compounds form energetically stable and perfectly crystalline closed-cage structures by folding the molecular sheets into a nanotube. In the case of polyhedra of 2D

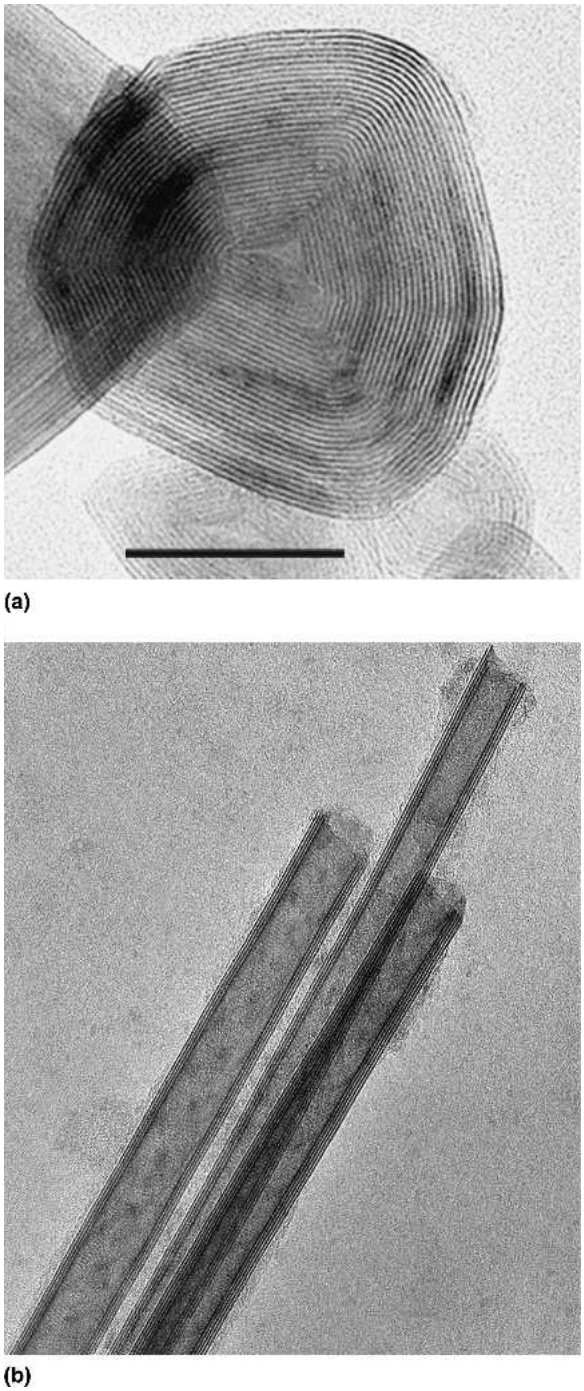

FIG. 2. (a) TEM image of a multi-wall MoS_2 fullerene-like particle with 30 closed layers. Scale bar is 20 nm. (b) Three WS_2 nanotubes 15–20 nm in diameter. The distance between each two layers is 0.61 nm. The *c* axis [001] is always normal to the surface of the nanotube.

compounds, they are obtained by introducing elements of lower symmetry, like pentagons or rhombi (squares) into the otherwise hexagonal (trigonal) lattice. Clearly, a pure 3D compound cannot form a perfectly ordered, flawless nanotubular or polyhedral structure by folding. The hollow nanotubes are obtained either by using a solid[13] or a

molten[14,15] template. The formation of true polyhedral—i.e., fullerene-like structures from 3D compounds, which require folding along two axes—is yet to be shown. Discommensuration is inevitable for a multilayered folded structure like nanotubes because the number of atoms in each molecular sheet is different. Discommensuration can be accommodated in multilayer nanotubes of a 2D compound due to the easy shear of the molecular layers across each other. On the other hand, nanotubes of compounds with 3D structure can overcome the discommensuration by introducing dislocations, and hence the crystallinity of the nanotubes cannot be perfect in this case. Instead, nanotubes of 3D compounds with high crystalline order are frequently highly faceted.

Nanotubes of various kinds were synthesized in macroscopic amounts, which permitted systematic studies of their properties and proposing novel applications for such nanostructures. Among them one can find WS_2,[16,17] MoS_2,[18] BN,[19] V_2O_5,[20] and $H_2Ti_3O_7$.[21] However, by all means the successful synthesis of multiwall nanoparticles of WS_2[22] and MoS_2[23] with closed-cage (fullerene-like) structure was the most rewarding accomplishment, in this respect. This phase is produced from the respective oxides in a pure form in quantities approaching a kilogram per day. In view of the large commercial potential, the production of this phase is expected to reach a few tons per day and above in the next few years. Generally, the synthesis of multiwall inorganic nanotubes or fullerene-like nanoparticles does not require a catalyst. Separation of a metal catalyst like nickel, which is mandatory for the growth of single-wall carbon nanotubes, is generally a tedious and a costly procedure.

Historically, interest in molecular structures with closed polyhedral and tubular form dates back to the work of Pauling, who investigated the mechanism of formation of tubular structures of asbestos minerals, like kaolinite.[24] Noted also for their tendency to form polyhedral structures are the boron-carbon-hydrogen compounds, the carbohydrenes which were investigated in great detail by Lipscomb.[25] However, the turning point came about when C_{60}[1] and, subsequently, carbon nanotubes[2] were discovered and gave birth to a new field of research in nanomaterials.

The mathematical theory of polyhedra made of a single layer is well established.[26] The geometrical analysis of polyhedra and nanotubular structures made of two and more interconnected layers has appeared only very recently, as a result of the discovery of the IF phases.[27–29] This development reflects the need to address the structure of nanotubes and polyhedral structures of inorganic layered materials. Such compounds consist of a stacking of molecular layers usually made of more than one kind of atom, with strong and oriented chemical bonds interconnecting the different atoms within the molecular sheet.

Of the list of important issues in this area, the making of size- and shape-selective clusters analogous to C_{60} is perhaps the most important and demanding one. It was found that different growth strategies led to inorganic fullerene-like nanoparticles and nanotubes with quite different structures. Each method produced nanotubes of different number of walls and chirality with size selectivity remaining an illusive target thus far. Some progress was reported in 2001 with the synthesis of bundles of single-wall MoS_2 nanotubes[30] using C_{60} as a growth promoter. However, so far this observation has not turned into a global strategy to synthesize singlewall MoS_2 nanotubes of any desirable diameter and chirality. Notwithstanding this preliminary report, single-wall nanotubes of no other metal dischalocogenide compound could be synthesized so far by a similar strategy. Laser ablation of MoS_2 and other metal dichalcogenide powders yielded multiwall MoS_2 octahedra.[31,32] These size- and shape-selective MoS_2 clusters are believed to play a role analogous to that of C_{60} in carbon clusters, which are discussed in greater detail below (Sec. II. F). It is likely that synthetic methods, like laser ablation and arc-discharge, which have played a primary role in the synthesis and elucidation of size-selective clusters of various compounds, will also leave their mark on the field of IF producing clusters with high degree of size and shape control.

The properties of inorganic nanotubes have not been studied in great detail until recently, when some remarkable studies demonstrated the great interest and potential applications of these nanomaterials. Theoretical calculations and optical measurements in the ultraviolet-visible (UV-vis) range provided important information regarding the electronic structure of these nanoparticles. Semiconducting nanoparticles generally exhibit a blue shift in the absorption and luminescence spectrum due to quantum size confinement of the electron (exciton) wavefunction. In contrast to that, the band gaps of semiconducting nanotubes like GaSe,[27] MoS_2,[28] SiC,[33] and numerous other nanotubes shrink with decreasing nanotube diameter. This effect is attributed to both zone folding and the strain in the folded structure. The latter phenomenon leads to a distortion of the chemical bonds and hence to a less efficient hybridization between the wave functions of the cation and anion wavefunctions in the lattice, i.e., closing the gap between the bonding and the nonbonding or antibonding orbitals. Furthermore, while armchair inorganic nanotubes were often found to have an indirect transition, zig-zag nanotubes possess a direct transition, suggesting that they could emit strong luminescence upon optical or electrical excitation. No experimental verification of these calculations was advanced so far.

The mechanical properties of inorganic nanotubes have been investigated in some detail in recent years. BN

nanotubes were shown to exhibit Young's modulus almost as high as that of carbon nanotubes.[34] The mechanical properties of individual WS_2 nanotubes have been investigated in detail using both experiment and theory.[35,36] These studies and others show that despite their smaller Young's modulus and larger specific weight compared to carbon nanotubes, inorganic nanotubes may find numerous applications in ultrahigh strength nanocomposites, mostly due to their high compression strength.

The numerous potential applications of inorganic nanotubes and fullerene-like nanoparticles are highlighted in a number of recent studies[37] and will be discussed in some detail below. Most importantly, IF-WS_2 and IF-MoS_2 were shown to exhibit superior tribological behavior to all known solid lubricants, particularly under high loads. This behavior offers a plethora of potential applications, which are being contemplated in joint development programs with major industrial manufacturers.

II. SYNTHETIC STRATEGIES

A. General

The synthesis of nanotubes from inorganic compounds has undergone a kind of explosive growth in recent years. Nanotubes of various inorganic compounds have been synthesized by a variety of methods. The availability of some of these nanotubes in large amounts permitted a systematic study into their physical and chemical properties. Large amounts of WS_2 and MoS_2 multiwall inorganic nanoparticles with fullerene-like structure[8,12,23] and various inorganic nanotubes have been realized.[14–20,38–40] Each of these techniques is very different from the others and produces nanotube and fullerene-like material of somewhat different characteristics. This fact by itself indicates that IF materials (including nanotubes) of 2D metal-dichalcogenides are a genuine part of the phase-diagram of the respective constituents. Of noticeable importance is the synthesis of bundles of iodine-doped single-wall MoS_2 nanotubes[30] and MoS_2 nanooctahedra.[31]

B. IF-MX_2 (M = transition metal; X = S, Se, Te)

One of the most successful synthetic methods that leads to highly crystalline MS_2 (M = Mo,W) nanotubes[30,39,40] is chemical vapor transport, a technique that was extensively used for the growth of high-quality single crystals of layered metal-dichalcogenides (MX_2) compounds. Here, MX_2 powder (or M and X elements in the 1:2 ratio) is placed on the hot side of an evacuated quartz ampoule, together with a halogen transport agent. A temperature gradient of 20–100 °C is maintained along the ampoule. After a few days, single crystal nanotubes or mixtures thereof are obtained on the colder side of the ampoule.

Synthesis of MoS_2 nanotubes using a solid template was also reported.[38] This synthesis is based on a generic deposition strategy, which was proposed by Martin and further perfected by Masuda and co-workers.[41] Nonuniform electrochemical corrosion of an aluminum foil in an acidic solution produces a dense pattern of cylindrical pores, i.e., anodic alumina oxide (AAO) membrane. This membrane serves as a solid template for the deposition of nanofilaments from a variety of materials. $(NH_4)_2MoS_4$ precursor was deposited from solution and annealed at 450 °C. The AAO membrane was dissolved in KOH, releasing a large amount of MoS_2 nanotubes. The limited thermal stability of the alumina membrane did not allow annealing temperatures higher than 500 °C, and consequently the crystallinity of the nanotubes was found to be quite poor. In fact, the MoS_2 nanotubes resembled more bamboo-like shaped hollow fibers.[38] More recently, numerous 1D nanostructures, like nanowires and nanotubes, were prepared using the AAO membrane as a solid template.

The growth mechanism of IF-MS_2 (M = Mo, W) materials by the sulfidization of the respective oxide nanoparticles has been elucidated in quite detail[8,12,23] and was also described in numerous papers and review articles. In brief, the initial step in this reaction is the sulfidization of the surface of the oxide nanoparticles at temperatures between 750 and 900 °C in an almost instantaneous reaction. This first sulfide layer passivates the nanoparticle surface and prevents coarsening of the nanoparticles into larger platelets. In the next slow step, the partially reduced oxide core is converted into metal-sulfide in a quasi-epitaxial layer by layer process, leading to a nested multilayer core.

The growth mechanism of IF-MoS_2 nanoparticles was elucidated using a three-region reactor, which permitted a good control over the growth parameters.[23] Here, the MoO_3 powder is heated to about 780 °C (Zone I, up). The volatile $(MoO_3)_3$ clusters are swept by the carrier gas (N_2) down until they cross the propagating front of the hydrogen molecules (Zone II, middle). The mild reduction conditions produce partially reduced MoO_{3-x} clusters, which are less volatile and therefore coalesce and form MoO_{3-x} nanoparticles. Once they grow to an adequate size (>5 nm), these suboxide nanoparticles react with H_2S gas. The mass difference between the two gases, which determines their diffusivity through the nozzles, is exploited to separate the reaction zones for the reduction and sulfidization in this zone (II). The sulfide coated oxide nanoparticles are carried by the gas outside the inner reactor and land on the ceramic filter (down), where the sulfidization reaction is completed.

Pure WS_2 nanotubes, 2–10 μm long and with diameters in the range of 20–30 nm, were reported by a number of groups.[16–18,42] An important intermediate phase in the conversion of WO_3 nanowhiskers into such

nanotubes is monoclinic $W_{18}O_{49}$ with pentagonal columns and hexagonal channels.[43] This phase provides a sufficiently stable but open structure for the sulfidization to proceed until the entire oxide core is consumed and converted into the respective sulfide.

Using a fluidized bed reactor (FBR), synthesis of multi-gram quantities of very long WS_2 nanotube phases was accomplished, however, not in a pure form.[44] The nanotubes obtained in this reaction are open ended, 15–20 nm in diameter, and 4–8 (WS_2) layers thick. They can be as long as a few hundred microns, very uniform in shape, with many of them having quite perfectly crystallinity, which is also manifested through their excellent mechanical behavior (vide infra).

One of the earliest syntheses of fullerene-like MoS_2 nanoparticles was made by electron beam irradiation of MoS_2 crystallites[45] and by microwave irradiation of a gas mixture containing the metal carbonyls.[46] Here, $Mo(CO)_6$ and $W(CO)_6$ powders were vaporized and then mixed with a heated H_2S(1%)/argon atmosphere under microwave irradiation. IF nanoparticles were formed when the reactor temperature was raised to 580 °C.

The synthesis of IF-MX_2 from the respective oxide nanoparticles suffers from a number of shortcomings. First, it was realized that some of the oxides, like those of titanium, tantalum, and niobium are very stable and do not lend themselves to a conversion into sulfide at temperatures below 1200 °C. Furthermore, the synthesis of IF-MX_2 from the respective metal oxides is a slow diffusion-controlled reaction. The product is strained, and consequently many defects occur in the closed fullerene-like nanoparticles. More recently, a new strategy has been adopted for the synthesis of IF-MS_2 and IF-MSe_2 nanoparticles using metal halides and carbonyls as precursors. These compounds have high vapor pressure already at temperatures not higher than 300 °C. Furthermore, they are very reactive with respect to H_2X vapor, forming MX_2 nuclei that is bound to grow very fast in the reaction atmosphere. The first successful synthesis using this approach was demonstrated for NbS_2.[47] Subsequently, open-ended TiS_2 nanotubes were synthesized by the reaction of $TiCl_4$ with H_2S.[48] In this kind of reaction, numerous nuclei are formed instantaneously due to the high exothermicity of the reaction and subsequently grow to nanotubes and nested nanoparticles through nucleation and growth mechanism.

In a recent report, fullerene-like TiS_2 nanoparticles with very high degree of crystallinity were obtained using $TiCl_4$ and H_2S as precursors.[49] The perfection of the nanoparticles topology was attributed to the use of a vertical reactor. Typical nanoparticles contain 80–120 layers; they are almost free of a hollow core and seem to be quite spherical in shape (see Fig. 3).

An interesting technique for the synthesis of MoS_2 nanoparticles with fullerene-like structure by the arc-discharge technique was reported as well.[50] Later on, an alternative version of this technique with the electrodes fully immersed in aqueous solution, which tames the reaction and leads to a better control of the reaction products, was also reported.[51]

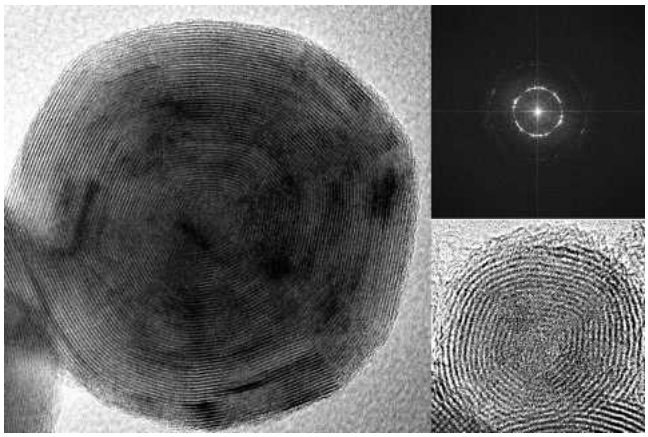

FIG. 3. TEM image of a typical IF-TiS_2 nanoparticle (left), produced in the vertical setup. The interlayer distance is 5.8 Å, and the diameter of the nanoparticle is larger than 70 nm. (Inset) The fast Fourier transform (FFT) of the shown nanoparticle. On the right, a small (20 nm) nanoparticle of the same kind is shown. Adapted from Ref. 49.

C. Metal oxide nanotubes via soft chemistry and other methods

Soft chemistry ("chemie douce") processes, like hydrothermal, sol-gel, intercalation reactions, sonochemical reactions, etc., play an ever larger role in the chemistry of inorganic compounds and nanomaterials, in particular. Early on, some remarkable synthesis of inorganic nanotubes through a sol-gel process, sometimes combined with hydrothermal or solvothermal methods, was reported.[20] In these reactions, a metal organic compound (e.g., a metal alkoxide) is dissolved first together with a template-forming species, like alkyl amine, in alcohol. In a certain concentration range, a soft template structure of hexagonally packed nanotubes array is formed. The addition of small amounts of water to the reaction vessel leads to a slow hydrolysis of the organic-metal compound, and a metal-oxide sol is thereby formed, retaining the template structure for the nanotubes. By tuning the pH, polycondensation of the metal oxi-hydroxide takes place and the sol transforms into a gel, which consists of a –M–O– polymer with longer chains. The process can be continued in a number of ways, leading eventually to metal oxide nanotubes.

Vanadium oxide nanotubes were obtained by first forming V_2O_5 sol, which was prepared by mixing vanadium (V) oxide triisopropoxide with hexadecylamine in ethanol. Aging the solution while stirring resulted in the hydrolysis of the vanadium oxide, which transformed into a gel.[20] Subsequently, a hydrothermal

treatment at 180 °C leads to the synthesis of nanotubes with the formal composition $VO_{2.45}(C_{16}H_{33}NH_2)_{0.34}$ (VO_x-alkylamine). Many of the nanotubes do not have a closed cap and in fact can be viewed as nanoscrolls rather than perfect nanotubes. The repeating motif in these nanotubes is made of two interconnected vanadate moieties and alkyl amine chain. Therefore, the spacing between the layers is determined by the sum of the inorganic and the organic part, which is generally 1.7–3.8 nm. Recently, VS_2 nanotubes were prepared by reacting VO_x-alkylamine nanotubes with H_2S.[52] This work is remarkable in so far as the bulk lamellar phase of VS_2 is not known.

In an early report, carbon nanotubes were used as templates for the deposition of V_2O_5 nanotubes; the solid template was subsequently removed by burning the sample in air at 650 °C.[53] This strategy can be easily adopted for the synthesis of different oxide nanotubes.

One of the most remarkable accomplishments of chemie douce processes in this field is the synthesis of what was initially believed to be TiO_2 nanotubes.[54,55] Such nanotubes may find a wide range of applications in photocatalytic processes, rechargeable batteries, smart glasses, solar cells, etc. The structure of these nanotubes was later shown to be related to the series of layered titanates, like $H_2Ti_3O_7$.[21] Careful inspection reveals that these nanostructures are in fact nanoscrolls, which is not surprising given the low temperatures used for the synthesis. Given the simple synthesis and the importance of titanium oxides for numerous applications, it is not surprising that recently a wave of studies has appeared on the titanate nanotubes.

A related family of compounds with layered structure is the oxychlorides. Recently the first nanotubular structures were prepared from the layered compound WO_2Cl_2 using chemie douce process.[56] They were probably formed by gradual exfoliation and restacking of the molecular slabs of the bulk compound.

Exfoliation of potassium hexaniobate-$K_4Nb_6O_{17}$ in the presence of alkyl amines led to the restacking of the films and formation of the niobate nanoscrolls.[57] Here, $K_{4-x}H_xNb_6O_{17}$ is obtained first by prolonged immersion of the precursor powder in 1 M HCl for several days. Subsequently aqueous solution of tetra(*n*-butyl)ammonium hydroxide was added to the solid while stirring until a stable value of pH = 10 was obtained. After sometime, an opalescent solution containing a colloid was obtained, which was analyzed after drying. The exfoliation process results in monomolecular layers, which fold and form closed nanotubes (nanoscrolls).

Layered structures are prevalent for hexavalent uranium oxo-compounds due to the strong tendency of the U^{6+} ion to form linear uranyl ions, UO_2^{2+}. The synthesis of an ordered array of $[(UO_2)_3(SeO_4)5]^{4-}$ nanotubes was recently reported.[58] The uranyl selenate nanotube array was obtained as small, greenish-yellow, transparent crystals from the room-temperature reaction of uranyl nitrate, K_2CO_3, and H_2SeO_4 in aqueous solution. It remains to be seen if the nanotubes can be separated into stable individual moieties.

A remarkable manifestation of the kinetic stabilization of closed fullerene-like nanostructures was demonstrated recently in the synthesis of tiny amounts of IF-Cs_2O nanoparticles.[11] Films of cesium oxides with approximately 2:1 Cs to O ratio and at monolayer-level dimensions are widely applied onto the surface of, e.g., S-1 photocathodes, negative electron affinity (NEA) devices, and also discharge lamps, television cameras, lasers, etc. These cesium oxide coatings were found to reduce the work-function of the electrode, thereby increasing the electron emission currents and the long wavelength response of these devices. Unfortunately, these films are highly reactive and they are damaged or destroyed by short exposure to low vacuum conditions. Powder of the layered compound 3R-Cs_2O closed in a sealed ampoule was laser ablated and subsequently inserted into the TEM through an air-tight environmental chamber (see Fig. 4). A few nested closed nanoparticles of Cs_2O were observed (Fig. 5). When taken out of the microscope, they

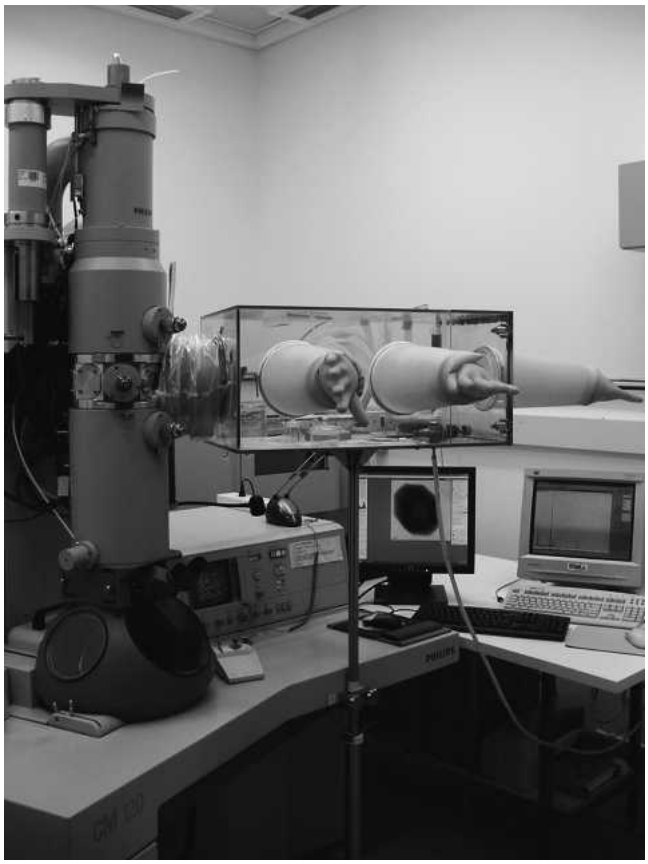

FIG. 4. Environmental chamber attached to the TEM enabling the transfer of ambient-sensitive samples.[4]

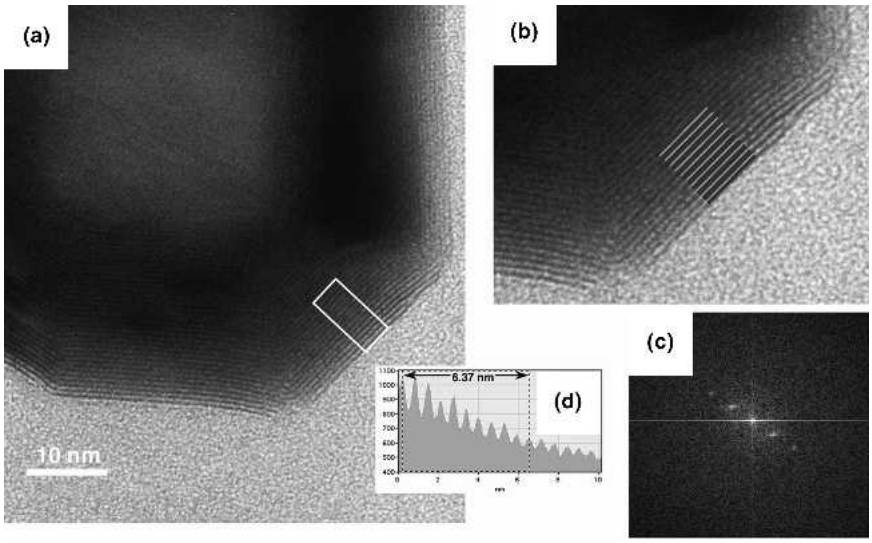

FIG. 5. TEM micrograph showing (a) blown-up view of a part of the IF-Cs_2O nanoparticle and (b) higher magnification of the IF-Cs_2O nanoparticle displayed in (a) with a computer simulation of the image overlaid on the lattice image. Note the good agreement between the simulated and experimentally observed image. (c) Fourier transform (FFT) of the framed area in (a). (d) line profile of the framed area in (a) showing an interlayer spacing of 6.37 Å. Adapted from Ref. 11.

showed a gradual exfoliation, but even after 1 h exposure, the inner layers of the fullerene-like nanoparticles remained intact though a small lattice expansion, probably due to partial water intercalation, took place. Examination of the physical properties and in particular the work function of the nanoparticles will not be possible unless larger amounts of the nanoparticles are available.

D. Metal halide IFs

Numerous metal halides, hydrates of metal-halides, and metal oxihalides are known to possess a layered structure and are therefore potential candidates for the synthesis of fullerene-like structures and nanotubes. In contrast to the metal dichalcogenides, which are very covalent in nature, the chemical bonds in the metal halides, and most particularly in the metal chlorides, are very polarized with a large density of electron cloud on the halide atom. Therefore, these compounds are in general very hygroscopic and in certain cases ($MgCl_2$) even deliquescent; i.e., they dissolve in their own water of hydration. The first demonstration for the kinetic stabilization of the IF structures was obtained with the layered compound $NiCl_2$. IF nanoparticles thereof were reported using, first, the sublimation-condensation technique and, more recently, laser ablation.[5,6] Unfortunately, the synthesis of large amounts of these nanostructures proved to be rather difficult, mainly due to the hygroscopic nature of the compound. Thus no verification for the above hypothesis could be advanced.

$CdCl_2$ and its first hydrate $CdCl_2 \cdot H_2O$ are compounds with layered structure. $CdCl_2$ has a hexagonal structure with two $CdCl_2$ layers in the unit cell (2H). On the other hand, $CdCl_2 \cdot H_2O$ has a rhombohedral unit cell with three $CdCl_2 \cdot H_2O$ layers (3R). Irradiation of the 3R powder by the electron beam of a transmission electron microscope (TEM) leads to the loss of the water molecules and recrystallization of the powder into $CdCl_2$ nanoparticles with closed cage polyhedral structures.[59] Because bulk $CdCl_2$ is extremely hygroscopic, it is impossible to handle the bulk material in the ambient atmosphere. In contrast, the fullerene-like structures are perfectly stable in the ambient, which again is a manifestation of the kinetic stabilization of the closed-cage structures. IF nanoparticles of CdI_2 and $NiBr_2$ were also recently reported.

E. Nanotubes from nonlayered compounds

Early studies showed that quasi-isotropic 3D compounds yield mostly amorphous or polycrystalline nanotubes. These nanotubes were obtained, for example, by depositing a precursor on carbon nanotube-template followed by calcination. Using solid templates, like carbon nanotubes, nanowires, and AAO, or soft templates, like elongated micelles, various nanotubes of 3D compounds were obtained, however in poorly crystalline form.

Recent studies indicated that almost perfectly crystalline nanotubes of 3D compounds can be synthesized in a reproducible manner. Thus faceted GaN nanotubes with hexagonal cross section were obtained by the reaction of trimethylgallium and ammonia on an ordered array of ZnO nanowires, which served as a template.[13] The template was subsequently removed by thermal reduction

and evaporation of the zinc metal core. Carbothermal synthesis was used ingeniously to synthesize nanotubes of various 3D oxides, nitrides and sulfides. For example, in a reaction of this kind,[14,15,60] heated graphite was used to reduce a solid precursor M_2O_3 (M = Al,Ga,In), producing volatile intermediates—M_2O and CO—according to the proposed reaction:

$$M_2O_3(s) + 2C(s) \rightarrow M_2O(g) + 2CO(g) \quad . \qquad (1)$$

Subsequently, the intermediates reacted with nitrogen gas (ammonia) producing MN nanotubes with faceted cross section according to the reaction:

$$M_2O(g) + CO(g) \ + N_2 \rightarrow 2MN(NT) + CO_2(g) \quad . \qquad (2)$$

M_2O_3 (M = Ga, Al, In) nanotubes stuffed with M in their core were formed by a similar carbothermal reaction.[61] Here, the reduction of the metal oxide by the heated graphite occurs at elevated temperature. The molten metal M serves as a nucleus and template for furthering the nanotube's growth. Figure 6 shows faceted ZnS nanotubes with wurtzite lattice prepared in an induction oven at 1700 °C under water vapor pressure. The water vapor facilitated the chemical vapor transport by reacting with the graphite crucible forming a reactive reducing mixture of CO + H_2 gases.

It must be born in mind, however, that unlike nanotubes made of 2D (layered) compounds, which are inherently stable in the nano-range, those made from 3D compounds, like ZnS are not. Furthermore, the surfaces of nanotubes made of 3D compounds are not passivated and they often react with the ambient. Notwithstanding their limited stability, such nanotubes may exhibit rich phenomena and find numerous applications.

The rational synthesis of peptide based nanotubes by self-assembling of polypeptides into supramolecular structures was also demonstrated. This self-organization leads to peptide nanotubes, having hollow channels 0.8 nm in diameter and a few hundred nanometers long.[62] The connectivity of the proteins in these nanotubes is provided by weak hydrogen bonds. These structures benefit from the relative flexibility of the protein backbone, which does not exist in nanotubes of covalently bonded inorganic compounds. Self-assembly of a very short peptide, the Alzheimer's beta-amyloid diphenylalanine structural motif, led to the formation of discrete and stiff nanotubes.[63] These nanotubes are stabilized by the π-π interaction of the adjacent aromatic groups of the diphenylalanine.

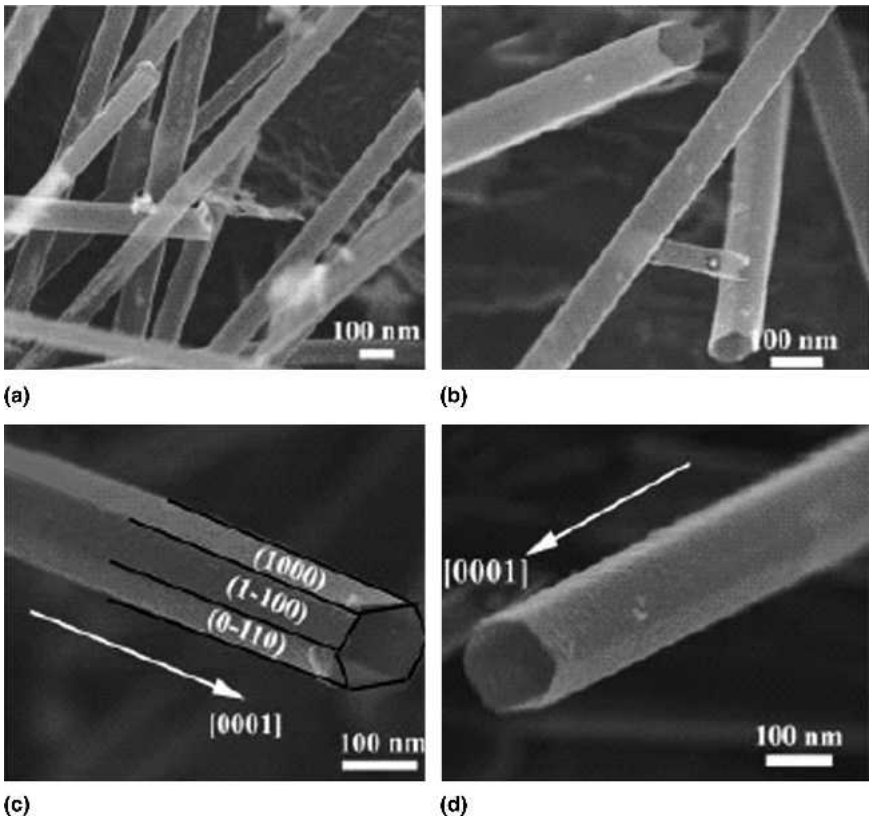

FIG. 6. SEM micrographs of ZnS nanotubes obtained by heating ZnS powder in graphite crucible in the presence of water vapor. The growth axis of the nanotubes is [001]. Adapted from Ref. 15.

F. Are there genuine inorganic fullerenes?

Carbon fullerenes are formed by a combination of hexagonal and pentagonal carbon rings. In particular, C_{60} is made of 20 hexagons and 12 pentagons. The formation of squares or even triangles is energetically not favorable for carbon. Most surprisingly, the formation of pentagonal rings with either B–B or N–N pairs as nearest neighbors is not favorable in $(BN)_n$ clusters either, although the B–N pair is isoelectronic to the C–C pair. Instead, closed-cage $(BN)_{12}$ made of 8 hexagonal rings and 6 squares arranged as symmetric octahederon was predicted to be the smallest stable, and thus genuine "fullerene," structure of BN.[64] Moreover, $(BN)_{24}$ nanoclusters made of 8 hexagons, 6 octagons, and 12 tetragonal rings were also synthesized and characterized.[65] In analogy to C_{60}, where no two pentagonal rings share a common edge, the tetragonal rings are also isolated. Similarly, one can ask himself what is the stable structure of the smallest hollow cage of MoS_2 or any other layered compound. If it exists, such a nanostructure would make the genuine "fullerene" of that compound.

Early on, it was suggested that layered compounds, like MoS_2, can form stable hollow cage structures made of a combination of hexagons and triangles or/and rhombi and arranged as a symmetric tetrahedron or octahedron, respectively.[7] The most compelling evidence in support of this idea was obtained in soot collected from laser-ablated MoS_2.[31] Nanooctahedra consisting of 2–4 layers [see Fig. 7(a)] with the inner one containing about 600 molybdenum and 1200 sulfur atoms, are routinely found in laser-ablated[32] and arc-discharge[51] MoS_2 samples. Schematic presentation of the Mo network in such a nanooctahedron is presented in Fig. 7(b). The rhombi in the corners of such nanooctahedra are clearly delineated.

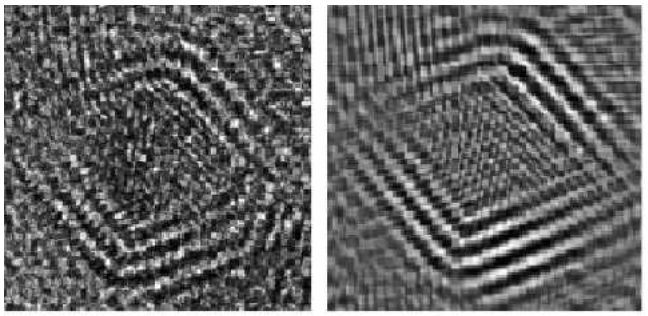

(a)

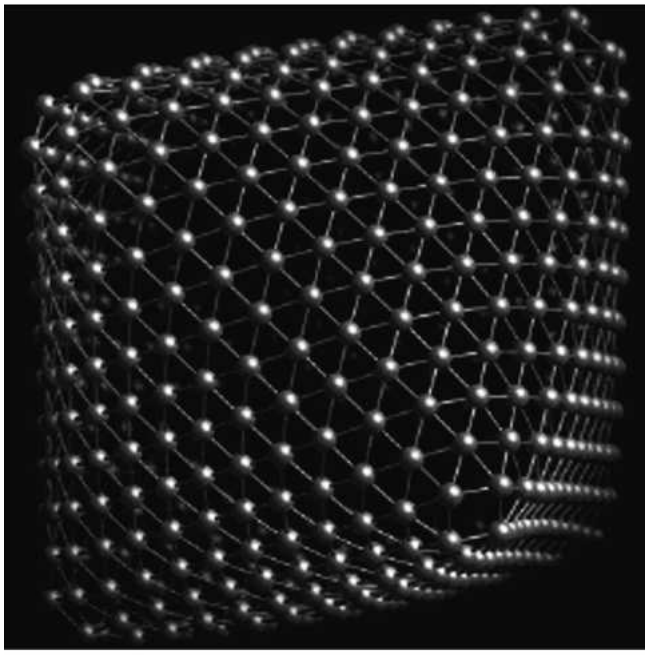

(b)

FIG. 7. (a) HRTEM image of a MoS_2 nanooctahedron produced by laser ablation (left) and its filtered image after FFT and back transform (right). (b) Schematic presentation of the molybdenum atoms arrangement in a MoS_2 nanooctahedron consisting of 572 Mo atoms.[32]

III. INORGANIC NANOTUBES STUDIED BY COMPUTATIONAL METHODS: ENERGETIC AND STRUCTURAL CONSIDERATIONS

With the advent of first-principles computational methods, analysis of nanotubes and fullerene-like structures from various inorganic compounds became possible, bringing new insight and predicting new properties, some of them yet to be verified by experiment. This section mainly addresses the stability aspects of inorganic nanotubes viewed from the perspectives of first-principles calculations. Further on, the same calculations are used to elucidate the electronic structure and the physical properties of such nanotubes. Early on Cohen, Louie, and their co-workers carried out an extensive effort to study the structure and the electronic structure of $B_xC_yN_z$ nanotubes.[66]

Further work of this group was carried out on nanotubes of the semiconducting layered compound GaSe.[27] In this compound, each atomic layer consists of a Ga–Ga dimer sandwiched between two outer selenium atoms in a hexagonal arrangement. The calculations demonstrated that the nanotubular structure is stable as compared to the same flat sheet of GaSe. The strain energy was shown to increase as $1/R^2$, where R is the radius of the nanotube. A more systematic approach to the study of the properties of inorganic nanotubes was undertaken by Seifert and co-workers using the density functional tight-binding (DFTB) approach. In a series of papers, semiconducting MoS_2[28] and metallic NbS_2[67] nanotubes were studied first, and their stability and properties were evaluated. The strain energy was found to increase as $1/R^2$. The structural stability of boron[68] and phosphorous[69] nanotubes and their electronic structure were studied. Black phosphorous (b-P) crystallizes in a hexagonal puckered

layered structure, in which the P–P bond distance is 2.23 Å with two bond angles of 102.8° and 96.58°. As with other layered materials, DFTB calculations have shown that b-P nanotubes are stable structures for tube diameter larger than 1.25 nm.

A computational effort was also made to elucidate the structure of putative nanotubes from nonlayered compounds (compounds with quasi-isotropic 3D structure). However, a clear dichotomy seems to exist between the experimental and the theoretical work. For example, faceted AlN nanotubes with wurzite (sp^3-like, i.e., 3D structure) lattice were synthesized[16] while graphitic (sp^2-like; 2D) lattice was postulated for the calculated AlN nanotubes.[70] Indeed, the calculated graphitic AlN nanotubes have strain energy higher by 0.68 eV/atom compared with cubic (sp^3-like) AlN materials. The elastic energy was found to be insensitive to the chirality of the sp^2-like AlN nanotube. Interestingly, the calculated graphitic AlN nanotubes were found to be stable when heated to 600 K, though they suffered some elliptical deformation. The first such nanotubes to be considered by DFT theoretical calculations were based on graphitic GaN.[71]

IV. PHYSICAL PROPERTIES

A. Band-structure calculations

Numerous publications have been dedicated to the calculations of the band structure of inorganic nanotubes. Early on, a few groups used first-principles theoretical tools to calculate the stability, band-structure, and other physical properties of $B_xC_yN_z$ nanotubes and fullerene-like nanoparticles. A few striking conclusions emerged from these studies. First, all BN nanotubes were found to be semiconductors (insulators), irrespective of their diameter or chirality. Secondly, while indirect band gap (Δ-Γ) was calculated for the armchair (n,n) nanotubes, the smallest forbidden gap of zig-zag (n,0) nanotubes was found to be a direct (Γ-Γ) one. Bulk BN material has an indirect band gap of 5.8 eV. These observations stand in sharp contrast with carbon nanotubes, which are either metallic or semiconducting, depending on their (n,m) values. Obviously, strain effects are predominant in nanotubes of small diameters. The distortion of the chemical bonds in the bent layer leads to shrinkage of the band gap of inorganic nanotubes. It is noticeable that the band gap of semiconducting carbon nanotubes increases with shrinking cage diameter. This trend could be attributed to the distortion of the C–C chemical bond, which is converted from mainly sp^2 (conductive) to sp^3 (insulating) character as the carbon nanotube diameter shrinks. Furthermore, it should be emphasized that generically, the band gap of semiconducting nanoparticles increases with decreasing particle diameter, a fact that is attributed to the quantum size confinement of the electron wavefunction.

The band structure of the GaSe nanotubes was also discussed.[27] The bulk material is a semiconductor with an indirect band gap of 2 eV. It was found that in analogy to BN and boro-carbonitride nanotubes, GaSe nanotubes are also semiconductors. In analogy to the previous observation with BN nanotubes, it was found here that the band gap shrinks with decreasing nanotube diameter.

First-principles calculations of single-wall MoS_2 and WS_2 nanotubes were also performed.[28] These studies confirmed the earlier observations, but they also went much further. While the lowest band gap of the armchair (n,n) nanotubes was found to be indirect, a direct transition was predicted for the zigzag (n,0) nanotubes. The strain energy was found to be almost one order of magnitude higher in these nanotubes as compared to carbon or BN nanotubes of the same diameter. The large difference in the strain energies of the various nanotubes was attributed to the appreciably larger thickness of the triple S-M-S layer (vide infra) as compared to the one-layer-thick carbon or BN nanotubes. Surprisingly, the band gap of many semiconducting nanotubes was shown to decrease with shrinking tube diameter.[28] These findings, which can be attributed to both strain effects and (Brillouin) zone folding, suggest a new mechanism for optical tuning in inorganic nanotubes. The existence of a direct gap in zigzag nanotubes is rather important because it indicates that such nanostructures may exhibit strong (electro)luminescence, which has not been observed for the bulk material. This theoretical observation needs to be confirmed experimentally.

Band-structure calculations of NbS_2 nanotubes showed that they exhibit a high density of states at the Fermi level, irrespective of their diameter or chirality.[67] This observation suggests that, while these nanotubes are metallic at room temperature, they may become superconductors at low temperatures. Similar behavior was observed for $NbSe_2$ and $Nb_{1.25}Se_2$ nanotubes. In another study, the same group carried out ab initio calculations for beta-zirconium nitrochloride (β–ZrNCl) nanotubes.[72] The bulk 2D compound is a semiconductor ($E_g = 1.6$ eV), which upon alkali metal intercalation becomes a superconductor with $T_c = 14$ K. In analogy to many other semiconducting nanotubes, the band gap of the armchair nanotubes shrinks with a decrease in their diameter. The effect of partial chlorine deintercalation on the electronic properties of β-$ZrNCl_{1-x}$-based nanotubes is also discussed. It was observed that, due to electron doping, the density of states at the Fermi level becomes very high, and the tubes transform into a metallic state, which could be significant for the appearance of superconductivity at low temperatures.

The space allocated for the present report does not permit a full account of the numerous theoretical and computational studies dedicated to nanotubes and fullerene-like structures. These studies provide a platform for the

comprehensive understanding of the structure and the physical properties of such nanostructures.

B. Transport properties

Fullerene-like MoS_2 nanoparticles (IF-MoS_2) and the powder of 2H–MoS_2 platelets were intercalated with sodium and potassium by exposing the powder to the vapor of the alkali metals. The chemical composition, structure, and transport properties of the non-intercalated and that of the alkali metal intercalated IF-MoS_2 and 2H–MoS_2 pellets were measured.[73] The intercalation was found to be inhomogeneous, and in general, the uptake of the alkali metal was faster and its concentration higher for the 2H than for the IF material. Exposure to the ambient atmosphere resulted in a gradual lattice expansion of the *c*-axis, i.e., increased layer to layer spacing, which was attributed to water uptake by the hydrated alkali atoms. After a few weeks of exposure to the ambient the hydrated alkali atoms diffused out of the MoS_2 leaving the IF nanoparticles almost unchanged. However, as expected, the rate of hydration and de-intercalation of the hydrated alkali metal from the MoS_2 lattice were found to be slower for the fullerene-like nanoparticles than that for the bulk powder. The alkali metal intercalated samples revealed a lower resistivity than the non-intercalated samples. Furthermore, magnetic measurements showed that whereas the non-intercalated samples were diamagnetic, the alkali metal intercalated samples became paramagnetic at low temperatures. The samples became highly resistant semiconductors and diamagnetic upon long exposure to the ambient, likely due to the deintercalation of the alkali atoms.

A recent work[74] described the fabrication and preliminary transport measurements of a superconducting InO nanowire deposited on top of a multiwall WS_2 nanotube. Quite surprisingly the nanotube itself is observed to be a good insulator, which is not expected for a semiconductor with a band gap of approximately 1.3 eV. Below 1 K, the InO superconductor nanowire exhibits magneto-electric oscillations; i.e., the resistance versus magnetic field shows distinct oscillations with a frequency of 8.5 $Tesla^{-1}$. These oscillations are reminiscent of the behavior underlying a superconducting quantum interference device.

C. Optical studies in the UV and visible and electronic excitations

In general, measurements of the optical properties in this part of the spectrum give information on the fundamental electronic transitions. The optical properties of IF-WS_2 nanoparticles, which were prepared by a careful sulfidization of oxide nanoparticles, were studied.[75] The excitonic nature of the optical transition in the nanoparticles was confirmed, which is a manifestation of the semiconducting nature of the material. A red shift of the fundamental transition (band gap) with shrinking radius of the IF nanoparticle was observed. Obviously, the exciton is mostly confined in the closed layer, and thus the quantum confinement is not expected to be very large. On the other hand, the elastic strain, which is imposed on the folded molecular sheets, induces the above red shift in the excitonic transitions.

In another study, the radius dependence of the fundamental transition of WS_2 nanotubes was evaluated both experimentally and by theoretical calculations.[76] Here a high-resolution scanning tunneling microscopy was used to image the WS_2 nanotubes and to analyze the density of states near the Fermi level. While the quality of the spectroscopic data was not satisfactory (see Fig. 8), the overall trend showing a red shift of E_g with shrinking radius of the nanotube was unequivocal, and the fit to the theoretical calculations was quite good. These observations suggest that band gap tuning by varying the nanotube diameter is possible, offering various applications for the IF phases, in photochromic, electrochromic, photoelectrochemical, and photocatalytic devices.

D. Raman spectroscopy

Raman and resonance Raman (RR) measurements of fullerene-like particles of MoS_2 have been carried-out.[77] Using 488-nm excitation from Ar ion laser light source, the two strongest features in the Raman spectrum of the crystalline particles, at 383 and 408 cm^{-1}, which correspond to the $E_{2g}{}^1$ and A_{1g} modes, respectively, were

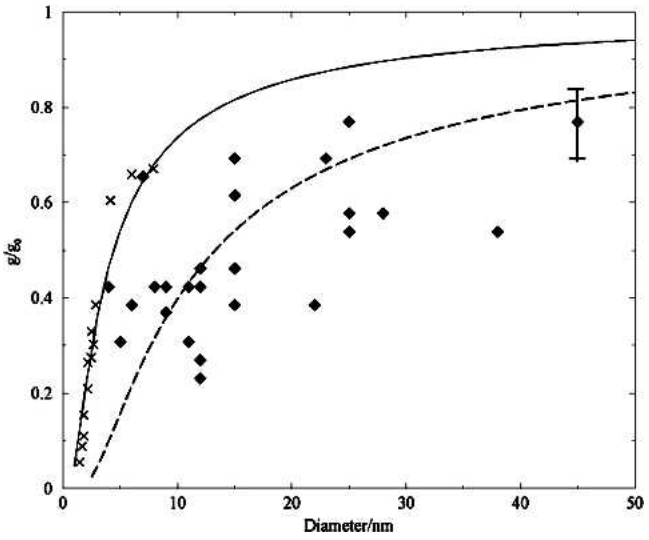

FIG. 8. The dependence of the band gap of WS_2 nanotubes as a function of their diameter (normalized to bulk WS_2). The diamonds are the experimental data obtained from STM measurements in the ambient. The crosses are values determined from first principle calculations. Note that both sets of data exhibit a decreasing band gap with shrinking diameter of the nanotubes.[75]

found to be dominant also in IF-MoS_2 and in MoS_2 platelets of a very small size. The broadening of these two features was attributed to the quantum confinement, which also leads to contributions of vibronic modes from the edge of the Brillouin-zone.

Polarized resonance Raman measurements of individual multiwall WS_2 nanotubes were recently described.[78] A strong Raman scattering signal was obtained when the light was polarized along the nanotube axis. Using a fit to a theoretical model, an estimate of the ratio of the perpendicular to parallel polarizabilities $\alpha_{XX}/\alpha_{ZZ} = 0.16$ was obtained, value of which is comparable to that obtained for single-wall carbon nanotubes (0.09). Symmetry analysis of the Raman and infrared (IR) active modes of MoS_2 nanotubes was also recently published.[79] The tubular structure is found to be characterized by two Raman active modes. A new high-energy breathing mode transition, which is characterized by the in-phase breathing of the sulfur shells and out of phase relative to the molybdenum atoms, was identified.

Raman studies of titania nanotubes[80] produced by the hydrothermal synthesis and VO_x-alkylamine nanotubes were undertaken.[81] These studies provided important structural information and were helpful in elucidating the mechanistic aspects of IF formation.

E. Mechanical properties

There is a surge of interest in measuring the mechanical properties of individual nanoparticles and in particular nanotubes and nanowires. This interest does not stem from pure academic reasons only but is driven by the search for new high performance nanocomposites. Nonetheless, the mechanical properties of inorganic nanotubes have been investigated to a relatively small extent so far. The Young's modulus of multi-wall BN nanotubes was measured individually within the TEM[34] and was estimated at 1.2 TPa, the value of which is comparable to the one measured for carbon nanotubes. A vertical array of dense and uniform GaN nanotubes was obtained on GaN substrate using the metalorganic chemical vapor deposition technique followed by plasma etching with reactive gases.[82] Buckling instability of the nanotubes was observed by nanoindentation. The Young's modulus (250–500 GPa) and the critical strain for buckling (8–22%) of the nanotubes were found to be both length and model dependent. Because the present nantoubes are made of a cubic GaN (sp^3 bonding lattice), any comparison with theoretical analysis that considers sp^2-bonded GaN nanotubes is questionable. Another difficulty stems from the fact that the present method does not allow for direct inspection of the nanotube during the buckling test.

A systematic experimental and theoretical study of the mechanical properties of individual WS_2 nanotubes is now underway. In the first work, the buckling of WS_2 nanotubes was followed using an atomic force microscope (AFM).[35] The experimentally determined force–displacement curve clearly showed a singularity point that was ascribed to the buckling of the nanotube. Using the Euler formula, the Young's modulus of the nanotubes was estimated at 170 GPa. First-principles theoretical calculations of the Young's modulus were found to be in agreement with the experimental data.

In a follow-up work, the mechanical properties of individual WS_2 nanotubes were measured within the scanning electron microscope (SEM). In situ tensile and buckling experiments were carried out.[36] Figure 9 displays a series of micrographs taken during the tensile test. The strain–stress curve of one such nanotube was thus obtained. The statistically averaged measured Young's modulus, strength, and elongation to failure were found to be 150 GPa, 16 GPa, and 12%, respectively. First-principles calculations were generally in agreement with the experimental findings. The experimentally determined strength of the WS_2 nanotubes is 11% of its Young's modulus, which is an exceedingly high value in comparison to high strength materials. It is important to realize that the onset of failure of the nanotubes emerges from excessive distortion of a chemical bond, while their role of macroscopic failure mechanisms, like dislocation/diffusion and propagation of cracks along grain boundaries, seems not to be applicable here.

Conceptually, nanomaterials of a high crystalline order are expected to show a remarkably different mechanical behavior as compared to macroscopic solids. The mechanical properties of regular solids are influenced by their intrinsic strength as well as the distribution of dislocations in the solid. Therefore, the strength of macroscopic objects is size dependent and is describable by the Weibull distribution. Figure 10 shows a SEM image of a post-buckled WS_2 nanotube. An average Young's modulus of 150 GPa was found by applying the Elastica theory to the present results, the value of which is consistent with all the previous measurements.[36]

In a series of works IF-WS_2 and IF-MoS_2 nanoparticles were shown to exhibit excellent resilience under shockwave pressures of 20–30 GPa with concurrent temperatures of up to 1000 °C. No evidence for significant structural degradation or phase change was observed, making these materials probably the strongest cage molecules known today and offering a plethora of applications.[83]

V. ELECTROCHEMICAL STUDIES

A. General

Electrochemical measurements are particularly pertinent to energy storage (intercalation batteries) and sensorial applications. Inorganic nanotubes could serve as

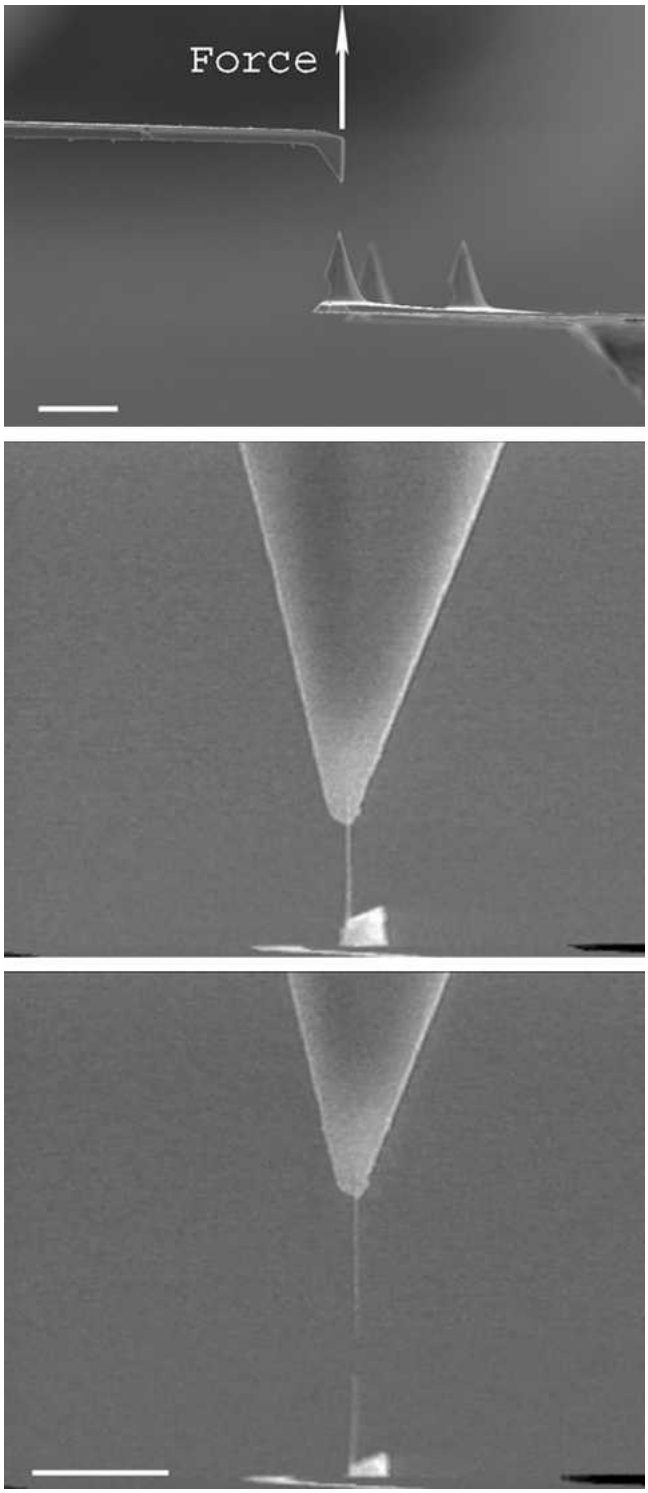

FIG. 9. Tensile test of an individual WS_2 nanotube carried-out within the SEM. The figure shows the nanotube before and after being torn apart. Adapted from Ref. 36.

hosts for the intercalation of both alkali metal and hydrogen atoms. The spacing between the layers, the hollow core in the center of the nanotube, and the voids between the densely packed nanotubes could be used to host guest atoms, with little if any disturbance to the pristine nanotube structure.

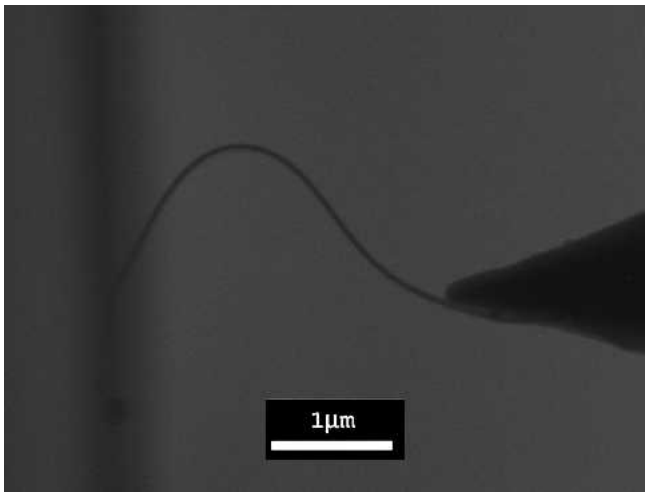

FIG. 10. SEM micrograph showing buckling of a WS_2 nanotube. Adapted from Ref. 36.

B. Li and hydrogen intercalation in MS_2 nanotubes

The electrochemical hydrogen-storage properties of the MoS_2 nanotubes were measured in an alkali electrolyte by a three-electrode system at 293 K.[84] The working electrode was prepared by pasting MoS_2 nanotubes onto a nickel-foam matrix. The counter-electrode was made of sintered $Ni(OH)_2$/NiOOH, and the reference electrode in this experiment was Hg/HgO. The cyclic voltammogram (CV) of the MoS_2 nanotubes electrode showed a cathodic peak at −0.955 V, which could be attributed to hydrogen reduction. The anodic peak observed at −0.645 V was assigned to hydrogen oxidation. The nanostructured MoS_2 electrode displayed a discharge capacity of 260 mAh/g (corresponding to the formula $H_{1.57}MoS_2$, i.e., 0.97 wt% hydrogen) at a current density of 50 mA/g and a temperature of 293 K. The electrode did not lose more than 2% of its original capacity after 30 consecutive charge/discharge cycles (100% depth of discharge at 150 mA/g to −0.6 V versus Hg/HgO).

Adsorption/desorption of hydrogen in MoS_2 nanotubes was also investigated at room temperature.[85] The hydrogen-adsorption kinetics is nearly linear, and it exhibits a saturation after about 30 min. Comparison of the gas adsorption (1.2 wt%) and electrochemical storage (0.97 wt%) suggests that the gas adsorption process is the result of a physisorption of the hydrogen in the MoS_2 nanotubes. The same group showed also that high-purity TiS_2 nanotubes with open-ended tips, which were synthesized by a chemical transport reaction, can efficiently store 2.5 wt% hydrogen at 298 K and under hydrogen pressure of 4 MPa.[86] Detailed analysis showed that about

1 wt% hydrogen is chemisorbed while the rest of the hydrogen atoms are physisorbed to the nanotubes.

Three moles of lithium could be inserted into $MoS_2I_{0.3}$ nanotube bundles, which were prepared by chemical vapor transport.[87] Comparing their electrochemical properties with those of bulk 2H–MoS_2, one finds a significant increase in the amount of inserted lithium and a decrease by about 0.7 V in the potential at which lithium insertion takes place for the electrodes made with the nanostructured material. The electron spin resonance (ESR) signal of lithiated $MoS_2I_{0.3}$ nanotube bundles was found to decrease upon exposure to the air but at a rate much slower than that of 2H–MoS_2 crystals, suggesting that lithiated $MoS_2I_{0.3}$ nanotube bundles are less air-sensitive than the lithiated bulk crystals.

C. Li intercalation in VO_x-alkylamine and titanate nanotubes

The synthesis of VO_x-alkylamine nanotubes by a sol-gel reaction and subsequent hydrothermal treatment has been described.[20] Further studies[88] have shown that these nanotubes could serve as high capacity Li insertion electrode. Gustafsson and co-workers were able to fabricate VO_x-alkylamine nanotube-based cathode with improved performance.[89] The electrode was tested by galvanostatic cycling in the potential range 1.8–3.5 V versus Li/Li^+. The capacities were found to be closely dependent on the type of lithium salt used in the electrolyte. Three salts were tested: $LiBF_4$, $LiPF_6$, and $LiN(CF_3SO_2)_2$. The imide salt $LiN(CF_3SO_2)_2$ gave the best result with initial capacities of 200 $mAhg^{-1}$. The electrode cycled reversibly for at least 100 cycles. X-ray diffraction results indicated that the tubular structure is preserved, even after prolonged cycling. In a related study, Whittingham and co-workers studied nanotubes of the partially metal-exchanged manganese compound $Mn_{0.1}V_{0.9}O_x$-alkylamine as electrode material for Li intercalation battery.[90] Li intercalation was studied also in titanate nanotubes.[91]

VI. APPLICATIONS

A. General

Starting from a preliminary report,[92] which demonstrated an improved tribological behavior for oils with IF as additives, numerous studies were focused on the applications of these nanostructures. The research work in this direction was summarized in a recent publication.[37] The reasons for these remarkable developments are 2-fold: (i) Synthetic strategies for large scale manufacturing of a few kinds of IF nanomaterials at affordable costs have been developed. (ii) Various observations suggested that IF materials possess interesting properties, making them suitable for applications in a variety of different domains—most significantly as solid lubricants and more recently as impact resistant materials in numerous systems. It was thus demonstrated that IF materials can be used as additives to improve the tribological behavior of lubrication fluids, greases, solid matrices impregnated with the nanoparticles, and self-lubricating coatings. Applications of a pure IF-MoS_2 powder could be envisioned in high vacuum and microelectronic equipment, where organic residues with high vapor pressure can lead to severe contamination. These advances have led to a surge of interest in this technology, and thus numerous development programs were undertaken with major industries. Some of these applications are already in use, while others are in a very advanced stage of development.

B. Tribological and impact resistant applications

In bulk 2H–MoS_2, molecular layers are held together by weak van der Waals forces. They can therefore easily shear with respect to one another and with respect to the two mating metal surfaces, which slide past each other. At the same time, the platelets serve as spacers, eliminating the direct contact between the two metal surfaces and thereby minimizing the metal wear. Therefore, MoS_2 powder is used as a ubiquitous solid-lubricant in various systems, especially under heavy loads, where fluid lubricants are squeezed out of the contact area between the two metal surfaces. Unfortunately, MoS_2 platelets tend to adhere to the metal surfaces through their reactive prismatic (*hk*0) edges, and their efficacy as solid lubricants is hampered. In contrast to that, the spherical IF-MS_2 nanoparticles are expected to behave like nano-ball bearings, and upon mechanical stress they would slowly exfoliate or mechanically deform but would not lose their tribological benefits until they are completely gone or until they oxidize. The beneficial effect of IF nanoparticles as a solid lubricant additive and in self-lubricating coatings has been confirmed through a long series of experiments in various research laboratories.[50,93–97]

The mechanism of the action of the IF nanoparticles as additives in lubricating fluids is more complicated than was initially thought. First, it is clear that the more spherical the nanoparticles and the fewer structural defects they contain, the better their performance is as solid lubricant additives. Early on, three main mechanisms responsible for the onset of failure of the nanoparticles in tribological tests were clearly identified: (i) exfoliation of the nanoparticles, (ii) deformation into a rugby ball shape, and (iii) puncturing and rupture under pressure and shear. The partially damaged (deformed) nanoparticles are left with reactive edges and dislocations, which can undergo further oxidation, gradually losing their tribological beneficial effect. Nanotribological experiments, using the surface force apparatus in which the IF-WS_2 lubricant was mixed with tetradecane between

two perpendicular mica surfaces, were carried out. These experiments revealed that material transfer from the IF nanoparticles onto the mica surface plays a major role in reducing the friction between two mica surfaces.[98] This phenomenon may have been responsible for the increased third body (slabs of WS_2) transfer observed in the experiments with the surface force apparatus.

More thorough investigation of the tribological action of the IF nanoparticles concluded that material transfer from the collapsing nanoparticles onto the mating mechanical surfaces plays a major role in reducing the friction and protecting the interface against excessive wear, particularly under heavy loads.[37,93]

Self-lubrication of mechanical parts can alleviate some of the technological complexities involved in the lubrication by fluids of mechanical systems, as well as relieving the environmental impact of this technology. For example, the use of fluid lubricants in the automotive industry adds some 2–3% to the overall weight of the cars. Adding 1% of the IF nanoparticles to the lubricating fluid could in fact lead to reduced size of the mechanical parts and therefore to considerable weight savings, although the nanoparticles themselves are somewhat heavier than most lubricating fluids. Furthermore, the technological complexities of these intricate systems impinge on their reliability, which could be substantially improved by adding 1% of the IF material. The used fluid lubricant must be processed or buried in special depots, which adds to the adverse environmental impact of automotive systems. Extending the lifetime of the mechanical parts in the car and the oil itself could therefore have an important environmental benefit.

C. Tips for scanning-probe microscopy

Another important field in which inorganic nanotubes can be useful is as tips in scanning-probe microscopy.[98] Here applications in the inspection of microelectronics circuitry have been demonstrated, and potential applications in nanolithography are being contemplated. Various inorganic nanotubes exhibit strong absorption of light in the visible part of the spectrum, and their electrical conductivity can be varied over many orders of magnitude by doping and intercalation. This suggests numerous possible applications in areas such as nanolithography, photocatalysis, sensors, and others. Recently, the technology of fabrication of such tips has been largely improved,[36] bringing this technology one step closer to a genuine application.

D. Optical, electrical and magnetic applications

This section deals with various studies that may show up as applications, but not in the very near future. Optical limiting behavior, i.e., opacity under high-intensity irradiation was observed in the visible and near-IR ranges in films produced from VO_x-alkylamine nanotubes.[99] Room-temperature ferromagnetic material was obtained by lithium and iodine intercalation of VO_x-alkylamine nanotubes.[100] The ferromagnetic behavior of the intercalated nanotubes' material was attributed to the lifting of spin frustration in the nanotube lattice, by either pairing (Li) or removal (I) of the highest occupied spin state. Furthermore, the lithium (iodine) doping brought the Fermi level into the conduction (valence) band, transforming this Mott–Hubbard insulator into a good conductor. This effect offers intriguing applications for such nanotubes in spintronics, memory devices, and sensors.

A number of interesting observations were made recently with titanate nanotubes. Thus, organic light emitting diodes mixed with titanate nanotubes were shown to exhibit stronger luminosity and lower the turn-on voltage.[101] It was suggested that the nanotubes lower the barrier for hole injection and improve the hole transport in the film. In another recent work, films made of titanate nanotubes exhibited enhanced electrochromism compared with films made of TiO_2 nanoparticles.[102] The nanotube films were prepared by alternating layer deposition of the negatively charged nanotubes and the positively charged polyelectrolyte onto a transparent conductive oxide glass. Subsequently, the polyelectrolyte was removed by photocatalytic oxidation using a UV light source. The titanate nanotube films exhibit a faster proton diffusion and higher proton capacity than those made of TiO_2 (anatase) nanoparticles. The significant electrochromism of the titanate nanotube film is attributed to its layered nanostructure. Finally, high-efficiency dye-sensitized solar cells were produced using single-crystalline titanate nanotubes as a thin-film semiconductor.[103] A very fast electron transfer rate through the single-crystalline titanate nanotubes films was observed as compared to that through nanoporous TiO_2 films composed of the normal nanoparticles. The dye-sensitized solar cells with single-crystalline titanate nanotubes showed more than doubling of the short-circuit current density than those made of titania nanoparticles (Degussa P-25) and overall solar to electrical conversion efficiency of 5%. Finally, arrays of titania nanotubes were prepared by electrochemical etching of titanium foil and used both as photoanodes for solar cells[104] and as sensors with very high sensitivity to hydrogen gas, with various possible medical applications.[105]

VII. CONCLUSIONS

Inorganic fullerene-like structures and inorganic nanotubes, in particular, are generic structures of nanoparticles of inorganic layered (2D) compounds. Various synthetic approaches to producing these nanostructures have been presented. In some cases, like WS_2, MoS_2, BN, and V_2O_5, both fullerene-like nanoparticles and nanotubes

are produced in gross amounts. However, size and shape control is still in its infancy. More recently, nanotubes of numerous inorganic compounds with nonlayered structure were prepared using various templates. Study of these novel nanostructures has led to the observation of a number of interesting properties and some potential applications in tribology, high energy density batteries, sensors, and nanoelectronics.

ACKNOWLEDGMENTS

This work was supported by the Israel Science Foundation. R.T. is the Director of the Helen and Martin Kimmel Center for Nanoscale Science of the Weizmann Institute and holds the Drake Family Chair in Nanotechnology. The IF-WS_2 material used for many of the recent experiments was provided by NanoMaterials, Ltd., Rehovot, Israel (www.apnano.com).

REFERENCES

1. H.W. Kroto, J.R. Heath, S.C. O'Brein, R.F. Curl, and R.E. Smalley: C_{60}: Buckminsterfullerene. *Nature* **318,** 162 (1985).
2. S. Iijima: Helical microtubules of graphitic carbon. *Nature* **354,** 56 (1991).
3. W. Krätschmer, L.D. Lamb, K. Fostiropoulos, and D.R. Huffman: Solid C_{60}—A new form of carbon. *Nature* **347,** 354 (1990).
4. R. Tenne, L. Margulis, M. Genut, and G. Hodes: Polyhedral and cylindrical structures of tungsten disulphide. *Nature* **360,** 444 (1992).
5. R.R. Chianelli, E.B. Prestridge, T.A. Pecoraro, and J.P. DeNeufville: Molybdenum disuflide in the poorly crystalline "Rag" structure. *Science* **203,** 1105 (1979).
6. J.V. Sanders: Structure of catalytic particles. *Ultramicroscopy* **20,** 33 (1986).
7. L. Margulis, G. Salitra, R. Tenne, and M. Talianker: Nested fullerene-like structures. *Nature* **365,** 113 (1993).
8. Y. Feldman, E. Wasserman, D.J. Srolovitz, and R. Tenne: High rate, gas phase growth of MoS_2 nested inorganic fullerenes and nanotubes. *Science* **267,** 222 (1995).
9. Y. Rosenfeld Hacohen, E. Grunbaum, R. Tenne, J. Sloan, and J.L. Hutchison: Cage structures and nanotubes of $NiCl_2$. *Nature* **395,** 336 (1998).
10. Y. Rosenfeld Hacohen, R. Popovitz-Biro, E. Grunbaum, Y. Prior, and R. Tenne: Vapor-liquid-solid (VLS) growth of $NiCl_2$ nanotubes via reactive gas laser ablation. *Adv. Mater.* **14,** 1075 (2002).
11. A. Albu-Yaron, T. Arad, R. Popovitz-Biro, M. Bar-Sadan, Y. Prior, M. Jansen, and R. Tenne: Closed-cage (fullerene-like) structures of Cs_2O. *Angew. Chem., Int. Ed. Engl.* **44,** 4169 (2005).
12. Y. Feldman, G.L. Frey, M. Homyonfer, V. Lyakhovitskaya, L. Margulis, H. Cohen, G. Hodes, J.L. Hutchison, and R. Tenne: Bulk synthesis of inorganic fullerene-like MS_2 (M = Mo, W) from the respective trioxides and the reaction mechanism. *J. Am. Chem. Soc.* **118,** 5362 (1996).
13. J. Goldberger, R. He, Y. Zhang, S. Lee, H. Yan, H.J. Choi, and P. Yang: Single-crystal gallium nitride nanotubes. *Nature* **422,** 599 (2003).
14. L.W. Yin, Y. Bando, Y.C. Zhu, M.S. Li, C.C. Tang, and D. Golberg: Single crytalline AlN nanotubes with carbon layer coating on the outer and inner surfaces via multiwall carbon nanotube-template-induced route. *Adv. Mater.* **17,** 213 (2005).
15. L.W. Yin, Y. Bando, J.H. Zhan, M.S. Li, and D. Golberg: Self-assembled highly faceted wurzite-type ZnS single-crystalline nanotubes with hexagonal cross-sections. *Adv. Mater.* **17,** 1972 (2005).
16. A. Rothschild, J. Sloan, and R. Tenne: The growth of WS_2 nanotubes phases. *J. Am. Chem. Soc.* **122,** 5169 (2000).
17. Y.Q. Zhu, W.K. Hsu, N. Grobert, B.H. Chang, M. Terrones, H. Terrones, H.W. Kroto, and D.R.M. Walton: Production of WS_2 nanotubes. *Chem. Mater.* **12,** 1190 (2000).
18. W.K. Hsu, B.H. Chang, Y.Q. Zhu, W.Q. Han, H. Terrones, M. Terrones, N. Grobert, A.K. Cheetham, H.W. Kroto, and D.R.M. Walton: An alternative route to MoS_2 nanotubes. *J. Am. Chem. Soc.* **122,** 10155 (2000).
19. J. Cumings and A. Zettl: Mass-production of boron nitride double-wall nanotubes and nanococoons. *Chem. Phys. Lett.* **316,** 211 (2000).
20. M.E. Spahr, P. Bitterli, R. Nesper, M. Müller, F. Krumeich, and H.U. Nissen: Redox-active nanotubes of vanadium oxide. *Angew. Chem., Int. Ed. Engl.* **37,** 1263 (1998).
21. G.H. Du, Q. Chen, R.C. Che, Z.Y. Yuan, and L.M. Peng: Preparation and structure analysis of titanium oxide nanotubes. *Appl. Phys. Lett.* **79,** 3702 (2001).
22. Y. Feldman, A. Zak, R. Popovitz-Biro, and R. Tenne: New reactor for production of tungsten disulfide hollow onion-like (inorganic fullerene-like) nanoparticles. *Solid State Sci.* **2,** 663 (2000).
23. A. Zak, Y. Feldman, V. Alperovich, R. Rosentsveig, and R. Tenne: Growth mechanism of MoS_2 fullerene-like nanoparticles by the gas phase synthesis. *J. Am. Chem. Soc.* **122,** 11108 (2000).
24. L. Pauling: The structure of the chlorites. *Proc. Natl. Acad. Sci. U.S.A.* **16,** 578 (1930).
25. N.N. Greenwood and A. Earnshaw: *Chemistry of the Elements* (Pergamon, Oxford, UK, 1990).
26. P.W. Fowler and D.E. Manolopoulos: *Ann. Atlas of Fullerenes* (Oxford University Press, Cambridge, UK, 1995).
27. M. Cote, M.L. Cohen, and D.J. Chadi: Theoretical study of the structural and electronic properties of GaSe nanotubes. *Phys. Rev. B* **58,** R4277 (1998).
28. G. Seifert, H. Terrones, M. Terrones, G. Jungnickel, and T. Frauenheim: Structure and electronic properties of MoS_2 nanotubes. *Phys. Rev. Lett.* **85,** 146 (2000).
29. A.N. Enyashin, N.I. Medvedeva, Yu.E. Medvedeva, and A.L. Ivanovskii: Electronic structure and magnetic states of crystalline and fullerene-like forms of nickel dichloride $NiCl_2$. *Phys. Solid State* **47,** 527 (2005).
30. M. Remskar, A. Mrzel, Z. Skraba, A. Jesih, M. Ceh, J. Demsar, P. Stadelmann, F. Levy, and D. Mihailovic: Self-assembly of subnanometer-diameter single-wall MoS_2 nanotubes. *Science* **292,** 479 (2001).
31. P.A. Parilla, A.C. Dillon, K.M. Jones, G. Riker, D.L. Schulz, D.S. Ginley, and M.J. Heben: The first inorganic fullerenes? *Nature* **397,** 114 (1999).
32. P.A. Parilla, A.C. Dillon, B.A. Parkinson, K.M. Jones, J. Alleman, G. Riker, D.S. Ginley, and M.J. Heben: Formation of nanooctahedra in molybdenum disulfide and molybdenum diselenide using pulsed laser vaporization. *J. Phys. Chem. B* **108,** 6197 (2004).
33. M. Zhao, Y. Xia, F. Li, R.Q. Zhang, and S.T. Lee: Strain energy and electronic structures of silicon carbide nanotubes: Density-functional calculations. *Phys. Rev. B* **71,** 085312 (2005).
34. N.G. Chopra and A. Zettl: Measurement of the elastic modulus of a multi-wall boron nitride nanotube. *Solid State Commun.* **105,** 297 (1998).

35. I. Kaplan-Ashiri, S.R. Cohen, K. Gartsman, R. Rosentsveig, G. Seifert, and R. Tenne: Mechanical behavior of WS_2 nanotubes. *J. Mater. Res.* **19,** 454 (2004).
36. I. Kaplan-Ashiri, S.R. Cohen, K. Gartsman, V. Ivanovskaya, T. Heine, G. Seifert, I. Kanevsky, H.D. Wagner, and R. Tenne: What makes the mechanical properties of (WS_2) nanotubes distinguishable from those of classical macroscopic objects. *Proc. Natl. Acad. Sci. U.S.A.* **103,** 523 (2006).
37. L. Rapoport, N. Fleischer, and R. Tenne: Applications of WS_2 (MoS_2) inorganic nanotubes and fullerene-like nanoparticles for solid lubrication and for structural nanocomposites. *J. Mater. Chem.* **15,** 1782 (2005).
38. C.M. Zelenski and P.K. Dorhout: Template synthesis of near-monodisperse microscale nanofibers and anotubules. *J. Am. Chem. Soc.* **120,** 734 (1998).
39. M. Remskar, Z. Skraba, F. Cléton, R. Sanjinés, and F. Lévy: MoS_2 as microtubes. *Appl. Phys. Lett.* **69,** 351 (1996).
40. M. Remskar, Z. Skraba, C. Ballif, R. Sanjinés, and F. Lévy: Stabilization of the rhombohedral polytype in MoS_2 and WS_2 microtubes: TEM and AFM study. *Surf. Sci.* **435,** 637 (1999).
41. H. Masuda and K. Fukuda: Ordered metal nanohole arrays made by a 2-step replication of honeycomb structures of anodic alumina. *Science* **268,** 1466 (1995).
42. Y.D. Li, X.L. Li, R.R. He, J. Zhu, and Z.X. Deng: Artificial lamellar mesostructures to WS_2 nanotubes. *J. Am. Chem. Soc.* **124,** 1411 (2002).
43. Y.Q. Zhu, W.K. Hsu, H. Terrones, N. Grobert, B.H. Chang, M. Terrones, B.Q. Wei, H.W. Kroto, D.R.M. Walton, C.B. Boothroyd, I. Kinloch, G.Z. Chen, A.H. Windled, and D.J. Frayd: Morphology, structure and growth of WS_2 nanotubes. *J. Mater. Chem.* **10,** 2570 (2000).
44. R. Rosentsveig, A. Margolin, Y. Feldman, R. Popovitz-Biro, and R. Tenne: WS_2 nanotube bundles and foils. *Chem. Mater.* **14,** 471 (2002).
45. M.J. Yacaman, H. Lopez, P. Santiago, D.H. Galvan, I.L. Garzon, and A. Reyes: Studies of MoS_2 structures produced by electron irradiation. *Appl. Phys. Lett.* **69,** 1065 (1996).
46. D. Vollath and D.V. Szabo: Nanoparticles from compounds with layered structures. *Acta Mater.* **48,** 953 (2000).
47. C. Schuffenhauer, R. Popovitz-Biro, and R. Tenne: Synthesis of NbS_2 nanoparticles with (nested) fullerene-like structure (IF). *J. Mater. Chem.* **12,** 1587 (2002).
48. J. Chen, S.L. Li, Z.L. Tao, and F. Gao: Low-temperature synthesis of titanium disulfide nanotubes. *Chem. Commun.* 980 (2003).
49. A. Margolin, R. Popovitz-Biro, A. Albu-Yaron, L. Rapoport, and R. Tenne: Inorganic fullerene-like nanoparticles of TiS_2. *Chem. Phys. Lett.* **411,** 162 (2005).
50. M. Chhowalla and G.A.J. Amaratunga: Thin films of fullerene-like MoS_2 nanoparticles with ultra-low friction and wear. *Nature* **407,** 164 (2000).
51. N. Sano, H. Wang, M. Chhowalla, I. Alexandrou, G.A.J. Amaratunga, M. Naito, and T. Kanki: Fabrication of inorganic molybdenum disulfide fullerenes by arc in water. *Chem. Phys. Lett.* **368,** 331 (2003).
52. H.A. Therese, F. Rocker, A. Reiber, J. Li, M. Stepputat, G. Glasser, U. Kolb, and W. Tremel: VS_2 nanotubes containing organic-amine templates from the NT-VO_x precursors and reversible copper intercalation in NT-VS_2. *Angew. Chem., Int. Ed. Engl.* **44,** 202 (2005).
53. P.M. Ajayan, O. Stephan, P. Redlich, and C. Colliex: Carbon nanotubes as removable templates for metal oxide nanocomposites and nanostructures. *Nature* **375,** 564 (1995).
54. P. Hoyer: Formation of a titanium dioxide nanotube array. *Langmuir* **12,** 1411 (1996).
55. T. Kasuga, M. Hiramatsu, A. Hoson, T. Sekino, and K. Niihara: Formation of titanium oxide nanotube. *Langmuir* **14,** 3160 (1998).
56. A.R. Armstrong, J. Canales, and P.G. Bruce: WO_2Cl_2 nanotubes and nanowires. *Angew. Chem., Int. Ed. Engl.* **43,** 4899 (2004).
57. G.B. Saupe, C.C. Waraksa, H-N. Kim, Y.J. Han, D.M. Kaschak, D.M. Skinner, and T.E. Mallouk: Nanoscale tubules formed by exfoliation of potassium hexaniobate. *Chem. Mater.* **12,** 1556 (2000).
58. S.V. Krivovichev, V. Kahlenberg, R. Kaindl, E. Mersdorf, I.G. Tananaev, and B.F. Myasoedov: Nanoscale tubules in uranyl selenates. *Angew. Chem., Int. Ed. Engl.* **44,** 1134 (2005).
59. R. Popovitz-Biro, A. Twersky, Y. Rosenfeld Hacohen, and R. Tenne: Nanoparticles of $CdCl_2$ with closed cage structure. *Isr. J. Chem.* **41,** 7 (2001).
60. L.Y. Yin, Y. Bando, D. Golberg, and M.S. Li: Growth of single crystal InN nanotubes and nanowires by controlled-carbonitridation reaction route. *Adv. Mater.* **16,** 1833 (2004).
61. J. Hu, Y. Bando, and Z. Liu: Synthesis of gallium filled gallium oxide-zinc oxide composite coaxial nanotubes. *Adv. Mater.* **15,** 1000 (2003).
62. M.R. Ghadiri, J.R. Granja, R.A. Milligan, D.E. McRee, and N. Khazanovich: Self-assembling organic nanotubes based on a cyclic peptide architecture. *Nature* **366,** 324 (1993).
63. M. Reches and E. Gazit: Casting metal nanowires within discrete self-assembled peptide nanotubes. *Science* **300,** 625 (2003).
64. F. Jensen and H. Toftlund: Structure and stability of C_{24} and $B_{12}N_{12}$ isomers. *Chem. Phys. Lett.* **201,** 89 (1993).
65. T. Oku, A. Nishiwaki, I. Narita, and M. Gonda: Formation and structure of $B_{24}N_{24}$ clusters. *Chem. Phys. Lett.* **380,** 620 (2003).
66. A. Rubio, J.L. Corkill, and M.L. Cohen: Theory of graphitic boron nitride nanotubes. *Phys. Rev. B* **49,** 5081 (1994).
67. G. Seifert, H. Terrones, M. Terrones, and T. Frauenheim: Novel NbS_2 metallic nanotubes. *Solid State Commun.* **115,** 635 (2000).
68. I. Boustani and A. Quandt: Nanotubules of bare boron clusters: Ab initio and density functional study. *Europhys. Lett.* **39,** 527 (1997).
69. G. Seifert and E. Hernandez: Theoretical prediction of phosphorus nanotubes. *Chem. Phys. Lett.* **318,** 355 (2000).
70. M. Zhao, Y. Xia, D. Zhang, and L. Mei: Stability and electronic structure of AlN nanotubes. *Phys. Rev. B.* **68,** 235415 (2003).
71. S.M. Lee, Y.H. Lee, Y.G. Hwang, J. Elsner, D. Porezag, and T. Frauenheim: Stability and electronic structure of GaN nanotubes from density-functional calculations. *Phys. Rev. B* **60,** 7788 (1999).
72. A.N. Enyashin, Yu.N. Makurin, and A.L. Ivanovskii: Electronic band structure of b-ZrNCl-based nanotubes. *Chem. Phys. Lett.* **387,** 85 (2004).
73. A. Zak, Y. Feldman, H. Cohen, V. Lyakhovitskaya, G. Leitus, R. Popovitz-Biro, S. Reich, and R. Tenne: Alkali metal intercalation of fullerene-like MS_2 (M = W, Mo) nanoparticles and their properties in comparison with bulk (2H) material. *J. Am. Chem. Soc.* **124,** 4747 (2002).
74. A. Johansson, G. Sambandamurthy, D. Shahar, N. Jacobson, and R. Tenne: Nanowire acting as a superconducting quantum interference device. *Phys. Rev. Lett.* **95,** 116805 (2005).
75. G.L. Frey, S. Elani, M. Homyonfer, Y. Feldman, and R. Tenne: Optical absorption spectra of inorganic fullerene-**l**ike MS_2 (M = Mo, W). *Phys. Rev. B* **57,** 6666 (1998).
76. L. Scheffer, R. Rosentzveig, A. Margolin, R. Popovitz-Biro, G. Seifert, S.R. Cohen, and R. Tenne: Scanning tunneling microscopy study of WS_2 nanotubes. *Phys. Chem. Chem. Phys.* **4,** 2095 (2002).
77. G.L. Frey, R. Tenne, M.J. Matthews, M.S. Dresselhaus, and

G. Dresselhaus: Raman and resonance Raman investigation of MoS_2 nanoparticles. *Phys. Rev. B* **60,** 2883 (1999). No.
78. P.M. Rafailov, C. Thomsen, K. Gartsman, I. Kaplan-Ashiri, and R. Tenne: The antenna effect in an individual WS_2 nanotube. *Phys. Rev. B* **72,** 205436 (2005).
79. E. Dobardziæ, B. Daki, M. Damnjanovic, and I. Milosevic: Zero *m* phonons in MoS_2 nanotubes. *Phys. Rev. B* **71,** 121405 (2005).
80. L. Qian, Z.L. Dub, S.Y. Yang, and Z.S. Jin: Raman study of titania nanotube by soft chemical process. *J. Mol. Struct.* **749,** 103 (2005).
81. W. Chen, L. Mai, J. Peng, Q. Xu, and Q. Zhu: Raman spectroscopic study of vanadium oxide nanotubes. *J. Solid State Chem.* **177,** 377 (2004).
82. S.C. Hung, Y.K. Su, T.H. Fang, S.J. Chang, F.S. Juang, L.W. Ji, and R.W. Chuang: Buckling instabilities in GaN nanotubes under uniaxial compression. *Nanotechnology* **16,** 2203 (2005).
83. Y.Q. Zhu, T. Sekine, Y.H. Li, M.W. Fay, Y.M. Zhao, C.H. Patrick Poa, W.X. Wang, R. Martin, P.D. Brown, N. Fleischer, and R. Tenne: Shock-absorbing and failure mechanism of WS_2 and MoS_2 nanoparticles with fullerene-like structure under shockwave pressures. *J. Am. Chem. Soc.* **127,** 16263 (2005).
84. J. Chen, N. Kuriyama, H.T. Yuan, H.T. Takeshita, and T. Sakai: Electrochemical hydrogen storage in MoS_2 nanotubes. *J. Am. Chem. Soc.* **123,** 11813 (2001).
85. J. Chen, S.L. Li, and Z.L. Tao: Novel hydrogen storage properties of MoS_2 nanotubes. *J. Alloys Compd.* **356–357,** 413 (2003).
86. J. Chen, S.L. Li, Z.L. Tao, Y.T. Shen, and C.X. Cui: Titanium disulfide nanotubes as hydrogen-storage materials. *J. Am. Chem. Soc.* **125,** 5284 (2003).
87. R. Dominko, M. Gaberscek, D. Arcon, A. Mrzel, M. Remskar, D. Mihailovic, S. Pejovnik, and J. Jamnik: Electrochemical preparation and characterization of Li_zMoS_{2-x} nanotubes. *Electrochim. Acta* **48,** 3079 (2003).
88. M.E. Spahr, P. Stoschitzki-Bitterli, R. Nesper, O. Haas, and P. Novak: Vanadium oxide nanotubes a new nanostructured redox-active material for the electrochemical insertion of lithium. *J. Electrochem. Soc.* **146,** 2780 (1999).
89. S. Nordlinder, K. Edstrom, and T. Gustafsson: The performance of vanadium oxide nanorolls as cathode material in a rechargeable lithium battery. *Electrochem. Solid-State Lett.* **4,** A129 (2001).
90. A. Dobley, K. Ngala, T. Shoufeng, P.Y. Zavalij, and M.S. Whittingham: Manganese vanadium oxide nanotubes: Synthesis, characterization, and electrochemistry. *Chem. Mater.* **13,** 4382 (2001).
91. J. Li, Z. Tang, and Z. Zhang: H-titanate nanotube: A novel lithium intercalation host with large capacity and high rate capability. *Electrochem. Comm.* **7,** 62 (2005).
92. L. Rapoport, Yu. Bilik, Y. Feldman, M. Homyonfer, S.R. Cohen, and R. Tenne: Hollow nanoparticles of WS_2 as potential solid-state lubricants. *Nature* **387,** 791 (1997).
93. L. Joly-Pottuz, F. Dassenoy, M. Belin, B. Vacher, J.M. Martin, and N. Fleischer: Ultralow-friction and wear properties of IF-WS_2 under boundary lubrication. *Tribol. Lett.* **18,** 477 (2005).
94. J.J. Hu and J.S. Zabinski: Nanotribology and lubrication mechanisms of inorganic fullerene-like MoS_2 nanoparticles investigated using lateral force microscopy (LFM). *Tribol. Lett.* **18,** 173 (2005).
95. R. Greenberg, G. Halperin, I. Etsion, and R. Tenne: The effect of WS_2 nanoparticles on friction reduction in various lubrication regimes. *Tribol. Lett.* **17,** 179 (2004).
96. W.X. Chen, Z.D. Xu, R. Tenne, R. Rosenstveig, W.L. Chen, H.Y. Gan, and J.P. Tu: Wear and friction of Ni–P electroless composite coating including inorganic fullerene-like WS_2 nanoparticles. *Adv. Eng. Mater.* **4,** 686 (2002).
97. Y. Golan, C. Drummond, J. Israelachvili, and R. Tenne: In situ imaging of shearing contacts in the surface forces apparatus. *Wear* **245,** 190 (2000).
98. A. Rothschild, S.R. Cohen, and R. Tenne: WS_2 nanotubes as tips in scanning-probe microscopy. *Appl. Phys. Lett.* **75,** 4025 (1999).
99. J.F. Xu, R. Czerw, S. Webster, D.L. Carroll, J. Ballato, and R. Nesper: Nonlinear optical transmission in VO_x nanotubes and VO_x nanotube composites. *Appl. Phys. Lett.* **81,** 1711 (2002).
100. L. Krusin-Elbaum, D.M. Newns, H. Zeng, V. Derycke, J.Z. Sun, and R. Sandstrom: Room-temperature ferromagnetic nanotubes controlled by electron or hole doping. *Nature* **431,** 672 (2004).
101. L. Qian, F. Teng, Z.S. Jin, Z.J. Zhang, T. Zhang, Y.B. Hou, S.Y. Yang, and X.R. Xu: Improved optoelectronic characteristics of light-emitting diodes by using a dehydrated nanotube titanic acid (DNTA)-polymer nanocomposites. *J. Phys. Chem. B* **108,** 13928 (2004).
102. H. Tokudome and M. Miyauchi: Electrochromism of titanate-based nanotubes. *Angew. Chem., Int. Ed. Engl.* **44,** 1974 (2005).
103. M. Adachi, Y. Murata, I. Okada, and S. Yoshikawa: Formation of titania nanotubes and applications for dye-sensitized solar cells. *J. Electrochem. Soc.* **150,** G488 (2003).
104. G.K. Mor, K. Shankar, M. Paulose, O.K. Varghese, and C.A. Grimes: Use of highly-ordered TiO_2 nanotube arrays in dye-sensitized solar cells. *Nano. Lett.* **6,** 215 (2006).
105. G.K. Mor, M.A. Carvalho, O.K. Varghese, M.V. Pishko, and C.A. Grimes: A room-temperature TiO_2-nanotube hydrogen sensor able to self-clean photoactively from environmental contamination. *J. Mater. Res.* **19,** 628 (2004).